

## Chaos and Periodicities in Solar Flare Index from Kandilli Observatory during 1976–2014

Soumya Roy<sup>1</sup>, Amrita Prasad<sup>2</sup>, Koushik Ghosh<sup>3</sup>, Subhash Chandra Panja<sup>2</sup> and Sankar Narayan Patra<sup>4</sup>

<sup>1</sup> Department of Applied Electronics and Instrumentation Engineering, Haldia Institute of Technology, Haldia, Midnapore (E) - 721657, West Bengal, India; [er.sroy9@gmail.com](mailto:er.sroy9@gmail.com)

<sup>2</sup> Department of Mechanical Engineering, Jadavpur University, Kolkata - 700032, West Bengal, India

<sup>3</sup> Department of Mathematics, University Institute of Technology, The University of Burdwan, Burdwan - 713104, West Bengal, India

<sup>4</sup> Department of Instrumentation and Electronics Engineering, Jadavpur University, Kolkata 700106, West Bengal, India; [sankar.journal@gmail.com](mailto:sankar.journal@gmail.com)

Received 2019 November 27; accepted 2020 February 26

**Abstract** The Solar Flare Index is regarded as one of the most important solar indices in the field of solar-terrestrial research. It has the maximum effect on Earth of all other solar activity indices and is being considered for describing the short-lived dynamo action inside the Sun. This paper attempts to study the short as well as long-term temporal fluctuations in the chromosphere region of the Sun using the Solar Flare Index. The daily Solar Flare Index for Northern, Southern Hemisphere and Total Disk are considered for a period from January 1976 to December 2014 (total 14 245 days) for chaotic as well as periodic analysis. The 0–1 test has been employed to investigate the chaotic behavior associated with the Solar Flare Index. This test revealed that the time series data is non-linear and multi-periodic in nature with deterministic chaotic features. For periodic analysis, the Raleigh Power Spectrum algorithm has been used for identifying the predominant periods within the data along with their confidence score. The well-known fundamental period of 27 days and 11 years along with their harmonics are well affirmed in our investigation with a period of 28 days and 10.77 years. The presence of 14 days and 7 days periods in this investigation states the short-lived action inside the Sun. Our investigation also demonstrates the presence of other mid-range periods including the famous Rieger type period which are very much confirming the results obtained by other authors using various solar activity indicators.

**Key words:** chaos — method: data analysis — Sun: activity — Sun: flares — Sun: fundamental parameters — Sun: rotation

### 1 INTRODUCTION

The Sun being a magnetically active star exhibits an 11 years solar activity cycle (half of the Hale cycle or 22 years magnetic cycle) due to the oscillation presented by various magnetic activities. The solar dynamo theory established that the magnetic field fluctuation within the convection zone is responsible for the dynamo process at the core of the Sun (Choudhuri 2007). The oscillatory nature of each and every stages of dynamo process is governed by the motion of the plasmas at different layers inside the Sun similar to radial localization (Stepinski & Levy 1991). The internal structure of the real Sun has more stages of dynamo process owing to the varying conditions of the convection

zone. The frequencies of oscillation at each stage of the dynamo process are well correlated with the variation of solar internal magnetic structure (Raychaudhuri 1971, 1972). Hence this should affect the characteristics of solar activities occurring in the chromospheric and coronal region of the Sun (Endal et al. 1985). Those dynamo processes at the Sun's core is responsible for apparent multi-periodic nature in a solar activity cycle (Boyer & Levy 1992).

The multi-periodic behavior of different solar activity indices like sunspot number as well as area, soft and hard X-ray flares index, 10.7 cm radio flux, coronal index, plage area etc. display frequencies ranging from days to decades (Lou 2000; Rybák & Dorotovič 2002; Bai 2003; Roy et al. 2019; Dimitropoulou et al. 2008; Chowdhury et al. 2009).

The well-known periods such as the 27 days rotational cycle and 11 years solar activity cycle is due to the monthly rotation and polarity interchange of the Sun's internal magnetic field respectively (Deng et al. 2015; Le & Wang 2003; Özgüç et al. 2002). The periods within these two well-known cycles (27 days and 11 years) can be found out by mid-term periodicity analysis, as it plays a very significant role in explaining the Solar magnetohydrodynamics (MHD) model (Bai 2003). Most significant mid-term periodicities are: (i) 154 days period which was first observed by Reiger in X-ray flare during 21st solar cycle (Rieger et al. 1984). This period was also found in other solar indices like hard X-ray peak rate (Bai & Sturrock 1987; Dennis 1985; Verma & Joshi 1987),  $H\alpha$  flare importance (Ichimoto et al. 1985), 10.7-cm radio peak flux (Kile & Cliver 1991; Roy et al. 2019) etc.; (ii) 84 days period was observed in flare data during solar cycle 20 (Bai & Sturrock 1991); (iii) 323 days periodicity was found in sunspot number as well as area (Oliver et al. 1992); (iv) 1.3 years periodicity was observed in geomagnetic activity (Mursula & Zieger 2000), solar wind oscillation (Richardson et al. 1994), solar wind velocity (Li et al. 2017), solar filament (Zou & Li 2014) and rate of internal rotation near base of the solar convection layer (Howe et al. 2000); (v) 1.7 years periodicity was found in the intensity of cosmic ray (Kato et al. 2003), velocity of solar wind (Li et al. 2017) and solar filament (Zou & Li 2014). The Sun also exhibits short-term (below 27 days) periodicity which mainly deals with spatial organization compare to temporal organization of the solar activity. Donnelly & Puga (1990) as well as Das & Nag (1999) reported a 14 days period which may be the sub-harmonic of the 28 days period. The presence of short-lived regions inside the Sun displayed a 7 days period (Donnelly & Puga 1990).

Many research on solar terrestrial domain established the fact that the solar flares have the maximum effect on Earth of all other solar activity indices (Özgüç et al. 2002). Yan et al. (2018) found that the solar flares are well correlated with solar magnetic fields. The Solar Flare Index is regarded as one of the most important solar indices in the field of solar-terrestrial research as it roughly represents the total emitted energy by a daily solar flare activity (Atac & Ozguc 1998; Kleczek 1952). For analyzing the fluctuation in the chromosphere region of the Sun, Solar Flare Index is considered as the best index among others. It displayed a good correlation with the other solar activities such as change in magnetic indices, sunspot number and sunspot area in photosphere region and also with the coronal variations (Atac & Ozguc 1998). So, the scientists and researchers around the world usually consider the Solar Flare Index as a powerful parameter for analyz-

ing and describing the short-lived dynamo action inside the Sun.

In earlier work (Roy et al. 2018), the Solar Flare Index was subjected to scaling analysis using the Finite Variance Scaling Method (FVSM) as well as Rescaled-Range Analysis (R/S). The Hurst Exponent (H) values obtained using R/S method were 0.033, 0.096, 0.099 whereas the values of H were 0.04, 0.104, 0.106 using FVSM for Solar Flare Index of Northern, Southern Hemisphere and Total Disk respectively. The reported analysis indicated the anti-persistent nature with Short Range Memory Dependency. It was also inferred that the time series data may have some hidden oscillation. This aspect has been further explored in this paper using two important attributes, i.e., Chaotic and Quasi-Periodic behavior of Solar Flare Index for Northern, Southern Hemisphere and Total Disk from 1976 to 2014 [Solar Cycle 21 – 24 up to 2014]. The considered data is subjected to chaos analysis using the 0 – 1 Test in order to search for the chaotic behavior. The Raleigh Power Spectrum method of spectrum analysis is used for finding the fundamental period along with their confidence level using the G R Quest method, ranging from short-term to long-term variation. The computed periods are also compared with the findings of other researchers with a similar type of data series.

## 2 DATA

This paper is primarily focused on computing fundamental periods of the daily Solar Flare Index (SFI) for Northern, Southern Hemisphere and Total Disk from January 1976 to December 2014 (total 14 245 days) [Solar Cycle 21 – 24 up to 2014]. The concept of Solar Flare Index was first discovered by Kleczek (1952) as  $SFI = it$  which is roughly proportional to the net emitted flare energy. In the above relationship,  $i$  symbolizes the scale of intensity and  $t$  represents the time span (in minutes) of flare in H-alpha flux. The computation of SFI is well explained by Özgüç et al. (2004) and the calculated data sets are available at the web page of the National Geophysical Data Center (NGDC) as well as at Kandilli Observatory. The plot of the daily SFI value for Northern, Southern Hemisphere and Total Disk are shown in Figure 1.

## 3 METHODOLOGY

### 3.1 0 – 1 Test for Chaos Analysis

The binary 0 – 1 chaos test was designed for deterministic systems in differentiating between chaotic and regular dynamics. This test was introduced and revised by Gottwald & Melbourne (2004, 2005) and does not depend on the phase plane reconstruction technique, which makes it unique over the widely used Lyapunov Exponent Method.

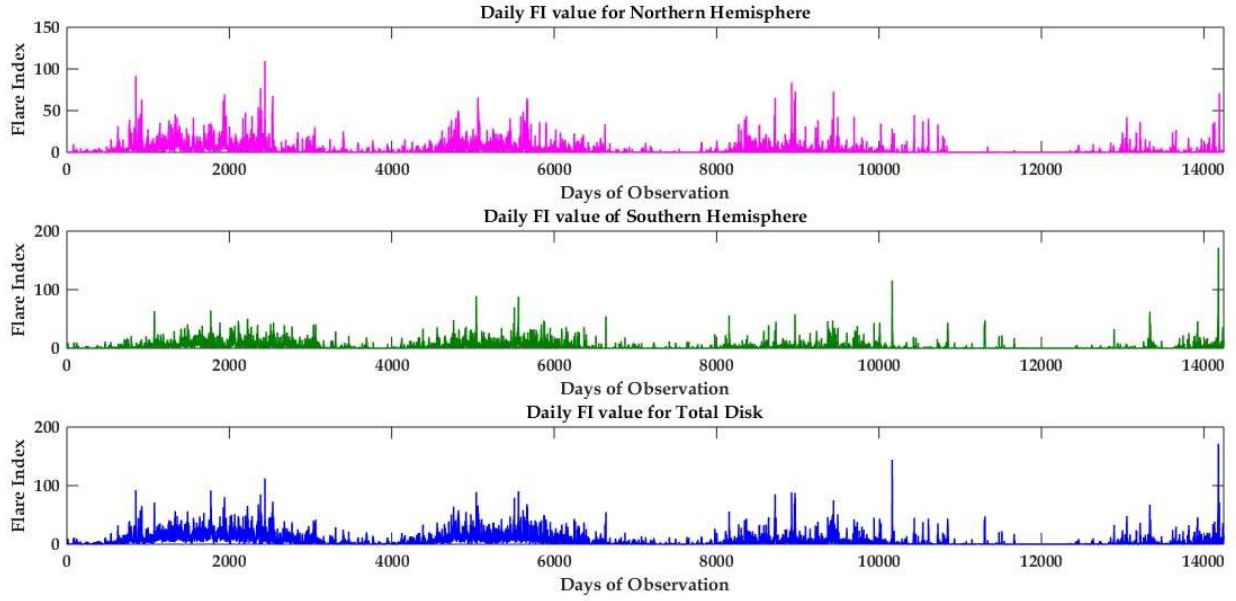


**Fig. 1** Variation of daily SFI value for Northern Hemisphere (purple), Southern Hemisphere (green) and Total Disk (blue) from January 1976 to December 2014 [Solar Cycle 21 – 24 up to 2014].

This test is also applicable for noisy and experimental (Falconer et al. 2007) time series data for detecting chaotic behavior. In this technique, the daily time series data is feed as an input and the obtained output is in the form of binary value which can minimize problems of distinguishing zero from small numbers. The binary value “1” or “0” represents that the time series data is “chaotic” or “non-chaotic” in nature respectively. The principal characteristics of this test are its robustness, reliability and easy implementation (Gottwald & Melbourne 2008). The test is implemented using time series data  $x(j)$  for  $j = 1, 2, \dots, N$  by the following steps (Gottwald & Melbourne 2009a):

1. Calculate the Fourier Transform variable of the time series data  $x(t)$  using the value of  $c$  within 0 to  $\pi$

$$P_C(n) = \sum_{j=1}^n x(j) \cos jc, \quad \text{and} \quad (1)$$

$$Q_C(n) = \sum_{j=1}^n x(j) \sin jc, \quad \text{for } n = 1, 2, \dots, N.$$

If a Brownian motion exists in  $P_C$  and  $Q_C$  plot then the time series data is “chaotic” in nature. On the other side, if a bounded motion exists in  $P_C$  and  $Q_C$  plot, then the time series data is “regular” or “non-chaotic” in nature.

2. The actual behavior of the Fourier Transform variable ( $P_C$  and  $Q_C$ ) can be scientifically examined by calculating the Mean Square Displacement  $D_C(n)$ . The test result is a bounded function with respect to time for “regular” or “non-chaotic” time series, whereas it

scales linearly with respect to time for “chaotic” time series. The Mean Square Displacement  $D_C(n)$  is computed as:

$$D_C(n) = \lim_{N \rightarrow \infty} \frac{1}{N} \sum_{j=1}^N [P_C(j+n) - P_C(j)]^2 + \lim_{N \rightarrow \infty} \frac{1}{N} \sum_{j=1}^N [Q_C(j+n) - Q_C(j)]^2. \quad (2)$$

The limit of  $n$  is ensured by computing  $D_C(n)$  only for  $n \leq n_{\text{cut-off}} \ll N$ . For better result, the practical value of  $n_{\text{cut-off}} = \frac{N}{10}$ . The value of  $c$  can be chosen in between 0 to  $\pi$ . A modified  $D_C(n)$  [ $MD_C(n)$ ] is used over normal  $D_C(n)$  for better convergence property. The  $MD_C(n)$  is computed by subtracting the explicit content  $V_{\text{OSC}}(c, n)$  from  $D_C(n)$  as follows:

$$MD_C(n) = D_C(n) - V_{\text{OSC}}(c, n), \quad (3)$$

where

$$V_{\text{OSC}}(c, n) = \left[ \lim_{N \rightarrow \infty} \frac{1}{N} \sum_{j=1}^N x(j) \right]^2 \frac{1 - \cos nc}{1 - \cos c}. \quad (4)$$

3. Compute the asymptotic growth [ $K_C$ ] by either regression or correlation method. The regression method can be applied on either  $D_C(n)$  or  $[MD]_C(n)$ . The result of regression method for  $D_C(n)$  is strictly positive whereas in case of  $[MD]_C(n)$ , the result may be negative depending on the value of  $V_{\text{OSC}}$ .

$$K_C = \lim_{n \rightarrow \infty} \frac{\log D_C(n)}{\log n}$$

or

$$K_C = \lim_{n \rightarrow \infty} \frac{\log[MD_C(n) - \min_{(n=1,2,\dots,n_{\text{cut-off}})} MD_C(n)]}{\log n} \quad (5)$$

4. Performed steps (1) to (3) for  $N_C$  number of different random value of  $c$  in between the range of 0 to  $\pi$ . In practice, the value of  $N_C$  should be 100 and more than that is sufficient. In this current investigation, 300 different random values are taken care of within the ranges of  $\frac{\pi}{5}$  to  $\frac{4\pi}{5}$  to overcome the resonance distortion of the statistics. Finally calculate the median of asymptotic growth [ $K$ ] of this test as follows:

$$K = \text{median}(K_c). \quad (6)$$

If the binary value  $K$  is zero or close to zero, then the time series data is “regular” or “non-chaotic” in nature. Similarly, if the binary value  $K$  is one or close to one, then the time series data is “non-regular” or “chaotic” in nature (Gottwald & Melbourne 2009b).

### 3.2 Raleigh Power Spectrum Algorithm for Periodicity Analysis

For a discrete time series data of continuously changing quantity, the periodicity can be analyzed by angular distribution of those discrete events using the Rayleigh Power Spectrum algorithm. In this method, each and every event is represented as a unit vector,  $\vec{v} = \cos \phi_i \hat{e}_x + \sin \phi_i \hat{e}_y$ , where  $\hat{e}_x$  and  $\hat{e}_y$  are two parallel unit vectors to the  $x$  and  $y$ -axes respectively. The sum of these unit vectors is

$$\vec{v}_i = \sum_{j=1}^L \cos \phi_j \hat{e}_x + \sum_{j=1}^L \sin \phi_j \hat{e}_y. \quad (7)$$

The calculation for uniformity of distributions is described by:

$$R = \frac{1}{L} \left[ \left( \sum_{j=1}^L \cos \phi_j \right)^2 + \left( \sum_{j=1}^L \sin \phi_j \right)^2 \right]^{\frac{1}{2}} \quad (8)$$

The value of  $R$  varies from zero to unity depending on whether events are distributed uniformly or concentrated around a particular angle. Furthermore, the value of  $Z$  for an event which is randomly distributed is defined as Bai & Cliver (1990):

$$Z = LR^2 = \frac{1}{L} \left[ \left( \sum_{j=1}^L \cos \phi_j \right)^2 + \left( \sum_{j=1}^L \sin \phi_j \right)^2 \right]. \quad (9)$$

The distribution of  $Z$  complies with  $P(Z > k) = \exp(-k)$  (Özgüç et al. 2003). The power spectrum is obtained by plotting  $Z(v)$  vs  $\phi_j = \frac{2\pi t_j}{T} = 2\pi v_j$ , where  $t_j$  is

set of occurrence time of the event and variable period is  $T$ .

Later, this algorithm was modified by considering each and every event as a modulus of vector  $|x(t_j)|$  instead of a simple unit vector as (Patra et al. 2009):

$$\vec{v}_i = \sum_{j=1}^L x(t_j) \cos \phi_j \hat{e}_x + \sum_{j=1}^L x(t_j) \sin \phi_j \hat{e}_y. \quad (10)$$

The vector sum and  $Z$  value are given by (Patra et al. 2009):

$$R = \frac{1}{L} \left[ \left( \sum_{j=1}^L x(t_j) \cos \phi_j \right)^2 + \left( \sum_{j=1}^L x(t_j) \sin \phi_j \right)^2 \right]^{\frac{1}{2}}, \quad (11)$$

$$Z = LR^2 = \frac{1}{L} \left[ \left( \sum_{j=1}^L x(t_j) \cos \phi_j \right)^2 + \left( \sum_{j=1}^L x(t_j) \sin \phi_j \right)^2 \right]. \quad (12)$$

Finally, ultimate analysis is obtained by plotting  $Z$  vs  $T$ .

### 3.3 Confident Peak Detection

#### 3.3.1 G R Quast method

The significance of any peak is decided by computing their confidence level using G R Quast method (Ferraz Mello & Quast 1987). The G R Quast method is applied to the signal after rescaling within 0 to 1 values. The confidence of the result (denoted by  $C$ ) is computed as follows:

$$C = (1 - e^{-H})^\alpha, \quad (13)$$

$$\alpha = \frac{2(N-3)\Delta t \Delta \omega}{3(N-4)}, \quad (14)$$

$$H = \frac{N-4}{N-3} (G + e^{-G} - 1), \quad (15)$$

$$G = - \left[ \frac{N-3}{2} \ln(1-S) \right], \quad (16)$$

where the time interval of the time series data for flare index is represented by  $\Delta t$  and the bandwidth of frequencies sampled is  $\Delta \omega$ . Also (1-confidence) may be interpreted as the chance of having the meridian of the highest peak only circumstantially.

#### 3.3.2 Sharpness test

A sharpness test was also performed on the given data to assure that the obtained peak falls within significant confidence level by using the following equation:

$$\max(f_l, f_r) < \alpha u, \quad (17)$$

where the amplitude of the considered peak is  $u$ ,  $f_l$  and  $f_r$  are the immediate minimum on both sides of the considered peak and  $\alpha$  is the significant level depending on the nature of periodogram. This test gives the sharp and confident peaks which are further considered in discerning the solar internal dynamics.

#### 4 RESULT AND DISCUSSION

The chaotic attributes associated with the Solar Flare Index of Northern, Southern Hemisphere and Total Disk are investigated using  $0 - 1$  test. Figure 2 represents  $Q_C$  vs.  $P_C$  in the complex plane,  $MD_c(n)$  versus  $n$  and  $K_c$  versus  $c$  for Solar Flare Index time series data.  $MD_c(n)$  versus  $n$  plot for Northern, Southern Hemisphere and Total disk Solar Flare Index represented for  $c$  is equal to  $\frac{1.59\pi}{5}$ ,  $\frac{1.13\pi}{5}$  and  $\frac{2.39\pi}{5}$  respectively.  $P_C$  versus  $Q_C$  plot for Northern, Southern Hemisphere and Total disk Solar Flare Index represented for  $c$  is equal to  $\frac{2.34\pi}{5}$ ,  $\frac{2.17\pi}{5}$  and  $\frac{2.05\pi}{5}$  respectively. The Fourier transform variables for Solar Flare Index time series data indicates a Brownian motion in the complex domain and modified mean square smoothed displacement  $MD_c(n)$  versus  $n$  plot scales linearly with respect to time. Also, the median of asymptotic growth  $[K]$  is 0.9977, 0.9979 and 0.9980 for Solar Flare Index of Northern, Southern Hemisphere and Total Disk respectively which is very close to binary value 1. According to the results of the  $0 - 1$  test, it can be concluded that the Solar Flare Index time series data is non-linear and multi-periodic in nature with deterministic chaotic features. However a question may arise at this point that how chaotic processes display multi-periodic features? Generally a chaotic process is nonlinear and aperiodic by nature. But a nonlinear system in a solar dynamo exhibits quasi-periodic behavior in time scale domain analysis due to the cyclic nature of the poloidal and toroidal components of the magnetic field (Cameron & Schüssler 2017, 2019).

The Solar Flare Index time series data is also subjected to periodicity analysis using the Raleigh Power Spectrum algorithm (Patra et al. 2009) for searching predominant periods. Figure 3 represents the periodogram profile of the Raleigh Power Spectrum algorithm at different ranges of periods. Several strong peaks with confidence level  $\geq 99\%$  using the G R Quast method (Ferraz Mello & Quast 1987) are being observed within the Solar Flare Index data. Also some periods within 96% – 99% confidence level are considered for this analysis to better understand of the different harmonics of fundamental periods. Among all observed periods, the significant periods are selected on the basis of the following selection criteria:

- For investigating intermediate mid-range periodicity, periods within  $\sim 7$  days to  $\sim 11$  years in Solar Flare

Index time series of Northern, Southern Hemisphere and Total Disk are considered.

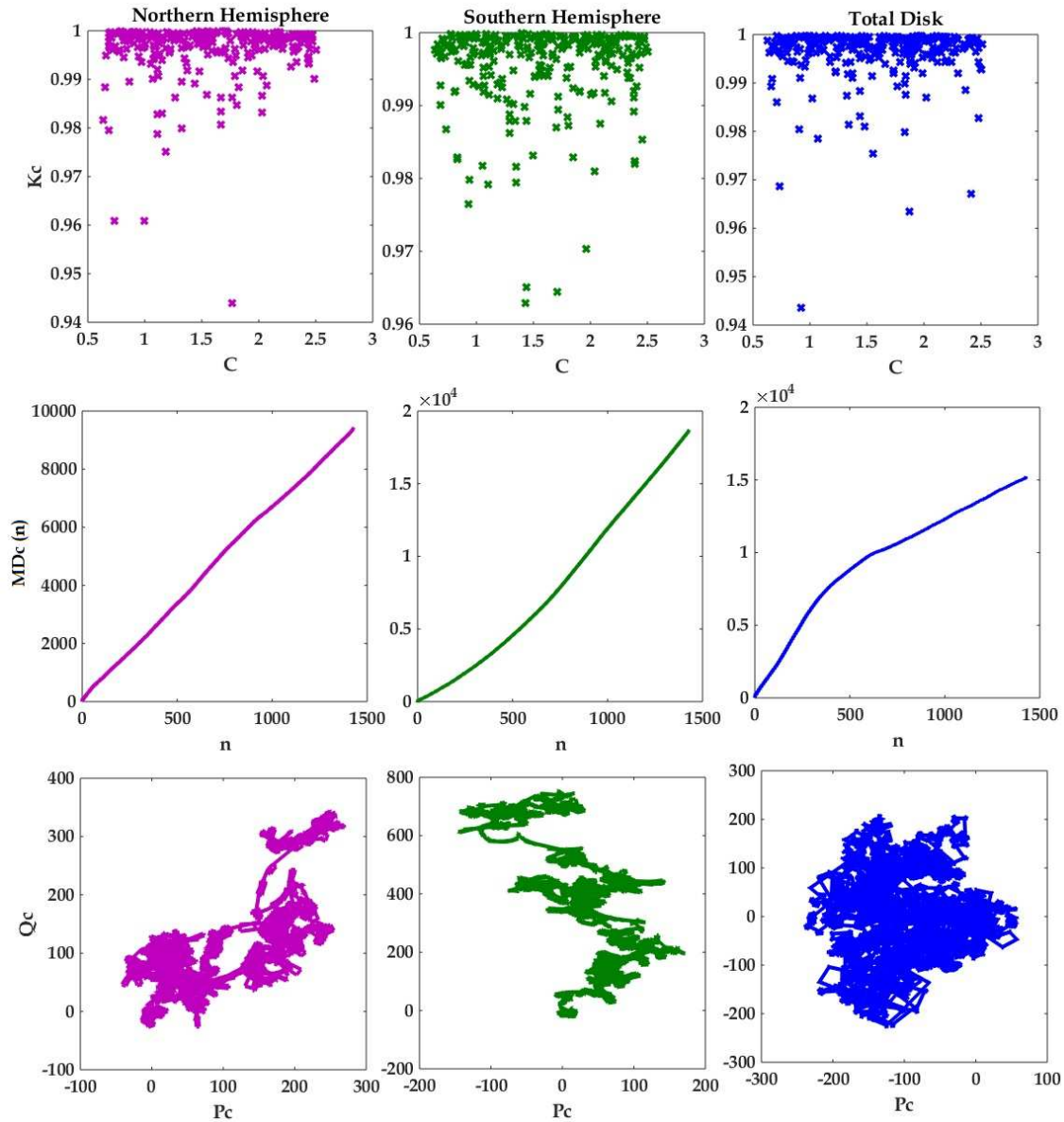
- Periods satisfying both confidence and sharpness test are being considered for further study.

Table 1 represents obtained significant periods within specified confidence band using the G R Quast method (Ferraz Mello & Quast 1987).

The periodogram methods have a significant and dominant period of about  $\sim 10.77$  years, which entails that the temporal fluctuation of the Solar Flare Index should be associated with the 11-years Schwabe cycle of various solar activity indices like sunspot number (Krivova & Solanki 2002; Li et al. 2005; Joshi et al. 2006; Kiliç 2008; Xie et al. 2017), group sunspot number (Li et al. 2005), sunspot area (Krivova & Solanki 2002; Joshi et al. 2006), Solar Radius (Qu et al. 2015), the soft X-ray flare index (Joshi & Joshi 2005), the flare index (Özgüç et al. 2003; Özgüç et al. 2004; Joshi et al. 2006; Kiliç 2008; Li et al. 2010), coronal mass ejection (CME) number (Lou et al. 2003), solar filament number (Li et al. 2006) and solar wind speed (Richardson et al. 1994). Another stable and prominent period of  $\sim 28$  days in Solar Flare Index of Northern, Southern Hemisphere and Total Disk was observed and which may be due to the existence of synodic rotational modulation (Xie et al. 2017). A prominent period of  $\sim 10.77$  years fluctuation is also eclipsed the other periods. In order to study the lower fluctuation more distinctly, the  $\sim 10.77$  years signal is filtered out (Kane 2005).

The short range periods (below  $\sim 28$  days) observed in this current investigation are  $\sim 7$  days and  $\sim 14$  days. Donnelly & Puga (1990) as well as Das & Nag (1999) reported that  $\sim 14$  days period is not only the sub-harmonic of  $\sim 28$  days period but is also due to the presence of  $180^\circ$  apart solar active longitudes. The  $\sim 7$  days period is nothing but the second harmonic of  $\sim 14$  days period primarily due to the presence of short-lived regions inside the Sun (Donnelly & Puga 1990). The periods of  $\sim 85$  days ( $28 \text{ days} \times 3 = 84 \text{ days}$ ) and  $\sim 311$  days ( $28 \text{ days} \times 11 = 308 \text{ days}$ ) are integral multiple of  $\sim 28$  days rotational modulation period. Also  $\sim 653$  days ( $10.77 \text{ years}/6 = 655 \text{ days}$ ) and  $\sim 1329$  days ( $10.77 \text{ years}/3 = 1311 \text{ days}$ ) are sub-harmonics of the  $\sim 10.77$  years fundamental Schwabe cycle.

Additionally, current investigation observed a period of  $\sim 152$  days which is very much similar to ‘Rieger periodicity’ [ $\sim 150 - 160$  days] which was first detected by Rieger et al. (1984) in soft X-ray flare and gamma ray data (around  $\sim 154$  days). After that many authors have reported the evidence of this periodicity in various solar activity indices such as sunspot numbers [ $\sim 158$  days (Ballester et al. 1999)], sunspot area [ $\sim 155$  days (Lean & Brueckner 1989; Carbonell & Ballester 1990)],  $\sim 158$  days (Oliver et al.



**Fig. 2**  $K_c$  versus  $c$  (top),  $MD_c(n)$  versus  $n$  (middle) and  $Q_c$  versus  $P_c$  (bottom) for Solar Flare Index.

**Table 1** Selected Periods from Periodogram Profile within Specified Confidence Band

Confidence level between 96% – 99%	Confidence level $\geq$ 99 %
14, 653, 1329 days	7, 28, 41, 85, 124, 152, 188, 238, 260, 311 days and 1.2, 1.76, 10.77 years

**Table 2** Comparison between Observed Periods and Periods due to Rossby Wave

Observed Periods	Periods due to magnetic Rossby wave		
	Node number	Wavenumber	Periods
41 days	01	03	41.92 days
124 days	01	10	126.8 days
188 days	01	15	189.1 days
238 days	01	19	239.1 days
260 days	01	21	264.2 days

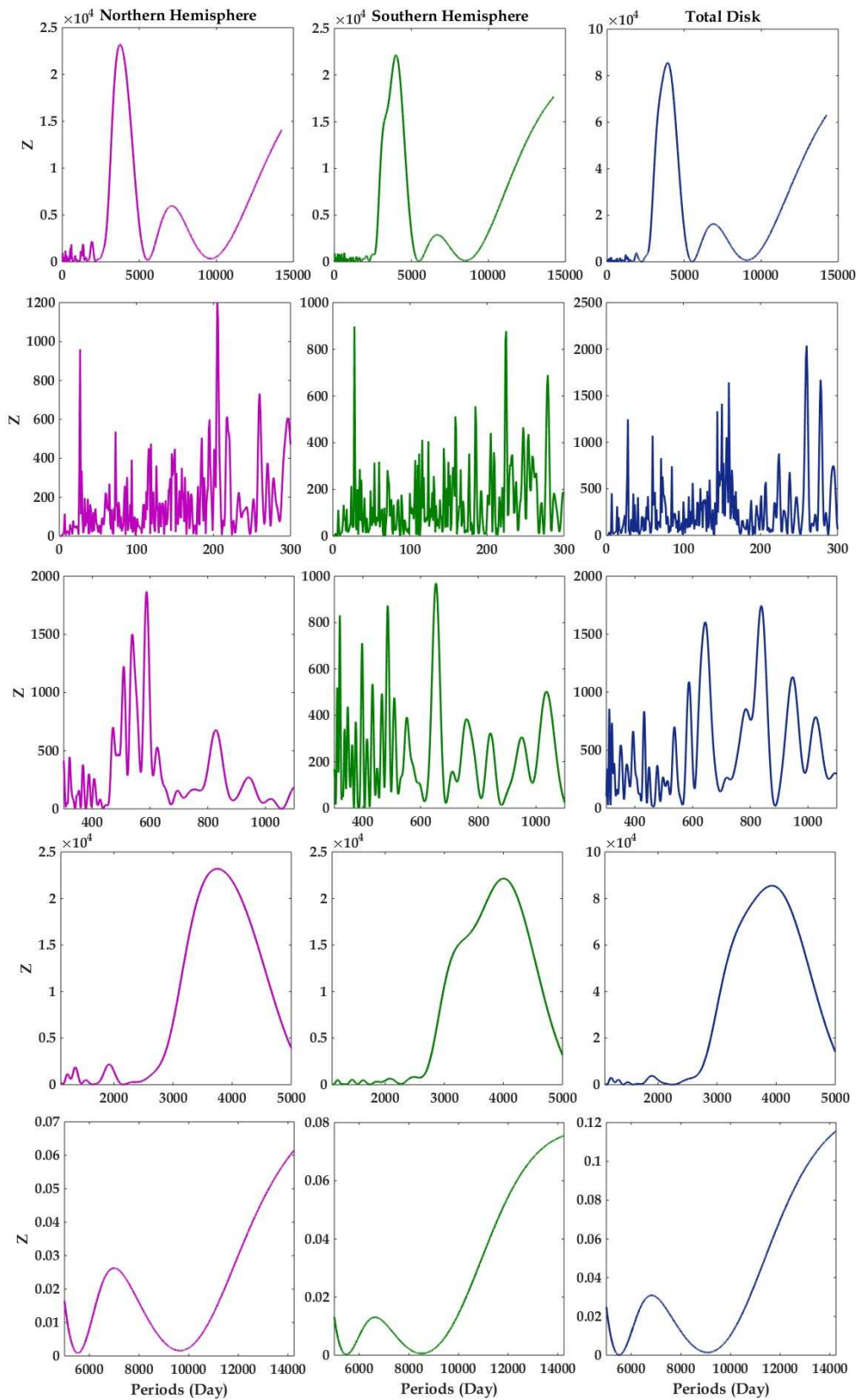


**Fig. 3** Periodogram profile for Solar Flare Index using Raleigh Power Spectrum Algorithm.

**Table 3** Comparison of the Result Derived by Other Authors with the Result of the Present Investigation using Solar Flare Index Data

Author Name	Data Source	Data Span	Tool Used	Period obtained	Observed Periods
Özgüç et al. (2003)	Kandilli Observatory and NGDC	January 1966 to July 2001	Discrete Fourier Transform and Wavelet Transform	27 days	28 days
Kiliç (2008)	Kandilli Observatory	August 1997 to December 2005	Date Compensated Discrete Fourier Transform	No significant periods	-
Gao et al. (2012)	Kandilli Observatory	1966 to 2007	Hilbert Huang Transform	11.8 years and 86.6, 191, 383, 865 days	10.77 years and 85, 188, 311 days
Özgüç et al. (2002)	Kandilli Observatory	1966 to 2002	Fourier Transform and Wavelet Transform	25.6, 27, 30.2, 33.8 days	28 days
Özgüç et al. (2004)	Kandilli Observatory	Solar cycle 23 up to December 2000	Fourier Transform and Wavelet Transform	35, 62, 116, 198, 276 days	88, 124, 188, 260 days
Li et al. (2010)	Kandilli Observatory	January 1996 to December 2007	Wavelet Transform	10.7 years	10.77 years
Kilcik et al. (2010)	Kandilli Observatory	Solar cycle 21 to 23	Wavelet Transform	27, 62, 73days	28, 88 days

1998; Chowdhury et al. 2009)], 10.7 solar radio flux [ $\sim 151$  days (Zieba et al. 2001);  $\sim 157$  days (Roy et al. 2019)], solar electron flare [ $\sim 156$  days (Chowdhury & Ray 2006)], hard X-ray emission [ $\sim 152 - 158$  days (Dennis 1985);  $\sim 152$  days (Bai & Sturrock 1987)], microwave peak flux [ $\sim 152$  days (Bogart & Bai 1985)],  $H\alpha$  importance [ $\sim 155$  days (Ichimoto et al. 1985)] etc. For identifying the source of ‘Rieger periodicity’, various attempts were made by authors and it was proposed that magnetic Rossby waves cornered in the surface of the Sun (Dimitropoulou et al. 2008; Zaqarashvili et al. 2010; Feng et al. 2017) may be the possible source behind this type of periodicity. The definition of typical magnetic Rossby waves for computing periodicity is expressed by Lou (2000):

$$P_{mrw} \cong 25.1 \left[ \frac{wn}{2} + \frac{0.17(2nn + 1)}{wn} \right] \text{ days}, \quad (18)$$

where  $wn$  and  $nn$  represent wavenumber and node number respectively. Current investigation also observed some periods ( $\sim 41, \sim 124, \sim 188, \sim 238, \sim 260$  days) due to magnetic Rossby waves with fixed node number ( $nn = 1$ ) and variable wavenumber ( $wn$ ). Table 2 lists the observed periods and similar periods due to magnetic Rossby wave.

A period of  $\sim 1.2$  years is found in our study which can be inferred to be the  $\sim 1.3$  years periodicity observed in geomagnetic activity (Mursula & Zieger 2000), oscillation in Solar wind (Richardson et al. 1994), velocity of solar wind (Li et al. 2017), solar filament (Zou & Li 2014) and rate of internal rotation near the base of the solar convection layer (Howe et al. 2000). On other hand  $\sim 1.76$  years period is related to the  $\sim 1.7$  years periodicity observed in the intensity of cosmic ray (Kato et al. 2003), velocity of solar wind (Li et al. 2017) and solar filament (Zou & Li 2014). These periods are also considered for understanding the behavior of magnetic field emergence and magnet-

ic cycle of the Sun (Valdés-Galicia et al. 1996). Cho et al. (2014) observed these two periods in the Earth’s magnetosphere, interplanetary space and on the Sun. They expected to detect a coupling nature among various region of the heliosphere but they found a relationship only between the Earth’s Magnetosphere and Interplanetary Space. Later on Deng et al. (2015) proposed that the process of magnetic field emergence from the Sun’s convection zone to heliosphere is periodic in nature, hence establishing the connection between the Sun and heliosphere. Mei et al. (2018) also found these periods in 10.7 cm solar radio flux as well as sunspot area data and suggested that the observed periods may be due to the flow of magnetic flux generated inside the Sun from the Sun’s photosphere to corona. Zou & Li (2014) suggested that the  $\sim 1.2$  years period may be one of the sub-harmonics ( $\frac{1}{8} \times 11 = 1.3$ ) of the dominant 11 years solar cycle. Li et al. (2017) also pointed out that the lifetime of the equilateral dipole field of the Sun is very close to the period around  $\sim 1.76$  years. These periods observed in the Solar Flare Index need further analysis to realize their connection among various regions of the heliosphere. The comparison between the different periodicity computed in the current investigation with periodicity related to other solar activity is presented in Table 3.

## 5 CONCLUSIONS

The daily Solar Flare Index is subjected to chaos analysis using  $0 - 1$  test. The median of asymptotic growth [ $K$ ] is 0.9977, 0.9973 and 0.9980 for the Solar Flare Index of Northern, Southern Hemisphere and Total Disk respectively which is very close to binary value 1. Also the Fourier transform variables for the considered data indicates a Brownian type motion in the complex domain and modified mean square smoothed displacement  $[MD]_c(n)$  ver-

sus n plot scales linearly with respect to time. So the 0 – 1 test indicates that the Solar Flare Index time series data has a deterministic chaotic features with multi-periodic nature. The periodicity analysis is applied to explore the quasi-periodic nature of Solar Flare Index. Hence the following list of periodicities has been obtained using the Raleigh Power Spectrum algorithm:

1. A significant and dominant period of about  $\sim 10.77$  years reveals that the temporal fluctuation of the Solar Flare Index should be well associated with the 11-years Schwabe cycle of the Sun. Another stable and prominent period of  $\sim 28$  days in Solar Flare Index of Northern, Southern Hemisphere and Total Disk can be interpreted as the existence of synodic rotational modulation. This investigation also observed some periods which are integral multiple of the  $\sim 28$  days rotational modulation period ( $\sim 85$  days and  $\sim 311$  days) as well as sub-harmonics of the  $\sim 10.77$  years fundamental Schwabe cycle ( $\sim 653$  days and  $\sim 1329$  days).
2. A period of  $\sim 14$  days is not only the sub-harmonic of the  $\sim 28$  days period but is also due to the presence of  $180^\circ$  apart solar active longitudes. The smallest period is  $\sim 7$  days which is nothing but the second harmonic of the  $\sim 14$  days period and is primarily due to the presence of short-lived regions inside the Sun.
3. A period of  $\sim 152$  days is very much similar to the ‘Rieger periodicity’ [ $\sim 150 - 160$  days]. Periods between  $\sim 40$  and  $\sim 300$  days are due to the magnetic Rossby wave which may be the possible source behind this ‘Rieger periodicity’.
4. A period of  $\sim 1.2$  years and  $\sim 1.76$  years observed with the data need further analysis for understanding the behavior of magnetic field emergence and magnetic cycle of the Sun.

**Acknowledgements** We are thankful to the National Geophysical Data Center (NGDC) and its sister data centers merged into the National Centers for Environmental Information (NCEI), NOAA. Data used in this study were provided by National Centers for Environmental Information for Solar-Terrestrial Physics, NOAA E/GC2, 325 Broadway, Boulder, Colorado 80303, USA.

We sincerely acknowledge the support extended by Jadavpur University, West Bengal India. This work is a part of RUSA 2.0 Faculty Major Research Project under Jadavpur University.

## References

- Atac, T., & iOzguc, A. 1998, *Solar Phys.*, 180, 397  
 Bai, T. 2003, *ApJ*, 591, 406  
 Bai, T., & Cliver, E. W. 1990, *ApJ*, 363, 299  
 Bai, T., & Sturrock, P. A. 1987, *Nature*, 327, 601  
 Bai, T., & Sturrock, P. A. 1991, *Nature*, 350, 141  
 Ballester, J. L., Oliver, R., & Baudin, F. 1999, *ApJ*, 522, L153  
 Bogart, R. S., & Bai, T. 1985, *ApJ*, 299, L51  
 Boyer, D. W., & Levy, E. H. 1992, *ApJ*, 396, 340  
 Cameron, R. H., & Schüssler, M. 2017, *ApJ*, 843, 111  
 Cameron, R. H., & Schüssler, M. 2019, *A&A*, 625, A28  
 Carbonell, M. and Ballester, J. L. 1990, *A&A*, 238, 377  
 Cho, I. H., Hwang, J., & Park, Y. D. 2014, *Solar Phys.*, 289, 707  
 Choudhuri, A. R. 2007, in *AIP Conf. Proc.*, 919, 49  
 Chowdhury, P., Khan, M., & Ray, P. C. 2009, *MNRAS*, 392, 1159  
 Chowdhury, P., & Ray, P. C. 2006, *MNRAS*, 373, 1577  
 Das, T. K., & Nag, T. K. 1999, *Solar Phys.*, 187, 177  
 Deng, L. H., Li, B., Xiang, Y. Y., & Dun, G. T. 2015, *JASTP*, 122, 18  
 Dennis, B. R. 1985, *Solar Phys.*, 100, 465  
 Dimitropoulou, M., Moussas, X., & Strintzi, D. 2008, *MNRAS*, 386, 2278  
 Donnelly, R. F., & Puga, L. C. 1990, *Solar Phys.*, 130, 369  
 Endal, A.S., Sofia, S., & Twigg, L. W. 1985, *ApJ*, 290, 748  
 Falconer, I., Gottwald, G. A., Melbourne, I., & Wormnes, K. 2007, *SJADS*, 6, 395  
 Feng, S., Yu, L., Wang, F., Deng, H., & Yang, Y. 2017, *ApJ*, 845, 11  
 Ferraz Mello, S., & Quast, G. R. 1987, *J Kleczek (ed.), Exercises in Astronomy*, 231  
 Gao, P. X., Xie, J. L., & Liang, H. F. 2012, *RAA (Research in Astronomy and Astrophysics)*, 12, 322  
 Gottwald, G. A., & Melbourne, I. 2004, *RSPSA*, 460, 603  
 Gottwald, G. A., & Melbourne, I. 2005, *PhyD*, 212, 100  
 Gottwald, G. A., & Melbourne, I. 2008, *PhRvE*, 77, 028201  
 Gottwald, G. A., & Melbourne, I. 2009a, *SJADS*, 8, 129  
 Gottwald, G. A., & Melbourne, I. 2009b, *Nonli*, 22, 1367  
 Howe, R., et al. 2000, *Sci.*, 287, 2456  
 Ichimoto, K., Kubato, J., Suzuki, M., Tohmura, I., & Kurokawa, H. 1985, *Nature*, 316, 422  
 Joshi, B., & Joshi, A. 2005, *Solar Phys.*, 226, 153  
 Joshi, B., Pant, P., & Manoharan, P. K. 2006, *A&A*, 452, 647  
 Kane, R. P. 2005, *Solar Phys.*, 277, 155  
 Kato, C., Munakata, K., Yasue, S., Inoue, K., & McDonald, F. B. 2003, *JGRA*, 108, 1367  
 Kilcik, A., Özgüç, A., Rozelot, J. P., & Ataç, T. 2010, *Solar Phys.*, 264, 255  
 Kile, J. N., & Cliver, E. W. 1991, *ApJ*, 370, 442  
 Kiliç, H. 2008, *A&A*, 481, 235  
 Kleczek, J. 1952, *Bull. Astron. Inst. Czech*, 3, 52  
 Krivova, N. A., & Solanki, S. K. 2002, *A&A*, 394, 701  
 Le, G. M., & Wang, J. L. 2003, *ChJAA*, 3, 391  
 Lean, J. L., & Brueckner, G. E. 1989, *ApJ*, 337, 568  
 Li, K. J., Gao, P. X., & Su, T. W. 2005, *Solar Phys.*, 229, 181  
 Li, K. J., Li, Q. X., Su, T. W., & Gao, P. X. 2006, *Solar Phys.*, 239, 493  
 Li, K. J., Gao, P. X., Zhan, L. S., Shi, X. J., & Zhu, W. W. 2010, *MNRAS*, 401, 342  
 Li, K. J., Zhang, J., & Feng, W. 2017, *MNRAS*, 472, 289

- Lou, Y. Q. 2000, *ApJ*, 540, 1102
- Lou, Y. Q., Wang, Y. M., Fan, Z., Wang, S., & Wang, J. X. 2003, *MNRAS*, 345, 809
- Mei, Y., Deng, H., & Wang, F. 2018, *Ap&SS*, 363, 84
- Mursula, K., & Zieger, B. 2000, *AdSpR*, 25, 1939
- Oliver, R., Carbonell, M., & Ballester, J. L. 1992, *Solar Phys.*, 137, 141
- Oliver, R., Ballester, J. L., & Baudin, F. 1998, *Nature*, 394, 552
- Özgülç, A., Ataç, T., & Rybák, J. 2002, *JGRA*, 107, 1146
- Özgülç, A., Ataç, T., & Rybák, J. 2003, *Solar Phys.*, 214, 375
- Özgülç, A., Ataç, T., & Rybák, J. 2004, *Solar Phys.*, 223, 287
- Patra, S. N., Bhattacharya, G., Ghosh, K., & Raychaudhuri, P. 2009, *Ap&SS*, 324, 47
- Qu, Z., Feng, W., & Liang, H. 2015, *RAA (Research in Astronomy and Astrophysics)*, 15, 879
- Raychaudhuri, P. 1971, *Ap&SS*, 13, 231
- Raychaudhuri, P. 1972, *Ap&SS*, 18, 425
- Richardson, J. D., Paularena, K. I., Belcher, J. W., & Lazarus, A. J. 1994, *GeoRL*, 21, 1559
- Rieger, E., et al. 1984, *Nature*, 312, 623
- Roy, S., Prasad, A., Chowdhury, S., Panja, S. C., & Patra, S. N. 2018, in *Proc. of IAU Symp.*, 340, 161
- Roy, S., Prasad, A., Panja, S. C., Ghosh, K., & Patra, S. N. 2019, *SoSyR*, 53, 224
- Rybák, J., & Dorotovič, I. 2002, *Solar Phys.*, 205, 177
- Stepinski, T. F., & Levy, E. H. 1991, *ApJ*, 379, 343
- Valdés-Galicia, J. F., Pérez-Enríquez, R., & Otaola, J. A. 1996, *Solar Phys.*, 167, 409
- Verma, V. K., & Joshi, G. C. 1987, *Solar Phys.*, 114, 415
- Xie, J. L., Shi, X. J., & Zhang, J. 2017, *ApJ*, 841, 1
- Yan, X. L., Wang, J. C., Pan, G. M., Kong, D. F., Xue, Z. K., Yang, L. H., Li, Q. L., & Feng, X. S. 2018, *ApJ*, 856, 79
- Zaqarashvili, T. V., Carbonell, M., Oliver, R., & Ballester, J. L. 2010, *ApJ*, 709, 749
- Zieba S., Maslowski, J., Michalec, A., & Kulak, A. 2001, *A&A*, 377, 297
- Zou, P., & Li, Q. X. 2014, *J. Geophys. Res. Space Phys.*, 119, 9357